IEEE Access
Multidisciplinary ⋮ Rapid Review ⋮ Open Access Journal

Received 2 March 2023, accepted 19 March 2023, date of publication 22 March 2023, date of current version 27 March 2023.

Digital Object Identifier 10.1109/ACCESS.2023.3260625

RESEARCH ARTICLE

Development of a Fuzzy Algorithm With Multiple Inputs for the Active Stabilizer Bar to Improve Vehicle Stability When Steering

TUAN ANH NGUYEN
Faculty of the Mechanical Engineering, Thuyloi University, Dong Da, Hanoi 100000, Vietnam
e-mail: anhngtu@tlu.edu.vn

ABSTRACT In this article, the author discusses the issue of vehicle roll instability when steering at high speeds. Installing an active stabilizer bar in a car is recommended to prevent it from rolling over and make it more stable when it does. A complex dynamic model is set up to evaluate and analyze vehicle oscillations. Besides, a fuzzy algorithm with three independent inputs is used to control the operation of the active stabilizer bar. This algorithm uses three separate inputs derived from the vehicle's oscillating signals. In addition, the membership function and fuzzy rule are designed to ensure that the quality and efficiency of the system are well-maintained and stable. This is an entirely new method, which is rarely used for complex models of cars. Numerical simulation is carried out in a Simulink environment with many specific cases and situations. According to research findings, the roll angle of the vehicle body increases as the speed increases. This causes a greater change in wheel dynamics force and increases the risk of rollover. If the car is equipped with an active stabilizer bar controlled by the fuzzy algorithm with three inputs, these problems are significantly reduced compared to all other situations. So, when this new algorithm is added to the active stabilizer bar, the car's stability and safety can improve even.

INDEX TERMS Active stabilizer bar, rollover phenomenon, fuzzy control, vehicle dynamic.

NOMENCLATURE

φ	Roll angle.
θ	Pitch angle.
α	Heading angle.
δ	Steering angle.
ψ	Yaw angle.
θ_m	Motor rotation angle.
a_y	Lateral acceleration.
F_{ASB}	Active stabilizer bar force.
F_C	Damping force.
F_K	Spring force.
F_{KT}	Tire force.
F_x	Longitudinal tire force.
F_y	Lateral tire force.
M_z	Aligning tire moment.
T_r	Resistance torque.
$u(t)$	Control signal.
v_x	Longitudinal velocity.
v_y	Lateral velocity.
X_{sv}	Servo valve displacement.
z_r	Road surface.
z_s	Sprung mass displacement.
z_u	Unsprung mass displacement.

The associate editor coordinating the review of this manuscript and approving it for publication was Jjun Cheng.

I. INTRODUCTION

When the vehicle is steering at high speed, phenomena associated with a roll and lateral instability may occur, such as a slip or rollover. The direct cause of these phenomena is centrifugal force, which causes the vehicle's body to tilt. Once the body is tilted, the difference in the dynamic forces between the two wheels will become apparent. The larger the body roll angle, the more significant the change in the wheel's vertical force will reduce the interaction between the wheel

and the road surface. Once the value of the wheel dynamics approaches zero, the wheel will be lifted off the road, and rollover phenomena may occur [1].

Vehicle lateral instability (including rollover) can occur with many vehicles, such as passenger cars, trucks, tank trucks, etc. [2], [3], [4]. Many subjective and objective causes cause lateral instability for cars moving on the road. In [5], Brandt et al. analyzed the instability of vehicles when traveling at high speeds, which is caused by crosswinds. Factors related to the vehicle's dimensions, such as the height of the center of gravity (CG), the wheelbase, the mass, etc., also significantly affected lateral instability when steering [6]. Besides, external factors such as the quality of the road surface or weather conditions also greatly influenced this problem [7], [8], [9]. Finally, factors that depend on the driver's use (steering angle, steering acceleration, speed, etc.) were the most critical factors involved in instability when moving. If the driver suddenly changes the direction of motion at high speed, lateral instability can quickly occur, as shown in [10]. Overall, the consequences of accidents involving lateral instability are immense.

Numerous researchers have published studies predicting lateral instability and rollover in the last few years. In [11], Nguyen has developed a new solution to determine the rollover limit of a car by using a 4-dimensional graph. According to the article's content [11], these graphs described the dependence between maximum roll angle, the distance from the CG to the RA (roll axis), velocity, and minimum vertical force. The idea of using a limited roll angle to evaluate the rollover phenomenon was also mentioned in [12] by Nguyen et al. There were many methods used to estimate and predict the vehicle roll angle, such as neural estimation in the MPC (model predictive control) system [13], an intelligent algorithm [14], a neural network [15], etc. In addition, several indicators that have been used to warn of lateral instability are also used, such as LTR (load transfer ratio) [16], [17] or RI (rollover index) [18]. These indicators were calculated using the difference between the dynamic forces of the wheels. In [19], Zhao et al. presented a new index called ZMP (zero moment point), which could also be used to predict the vehicle's lateral instability while steering. These indices could be transformed into a function that depends on the lateral acceleration, as demonstrated in [20] by Shin et al.

Wang et al. suggested using lateral stability control systems to make a car more stable while driving [21]. In [22], Sun et al. introduced the ADP (adaptive dynamic programming) algorithm for vehicle lateral stability using a linear double-track model. The system's control unit is designed indirectly to create impact forces that change the steering angle of the guide wheel. For heavy trucks, a complete control model has been developed based on the ideas of Jin et al. [23]. The electric motor's speed control, which is standard on electric vehicles, also aids rollover prevention [24]. In addition, roll and lateral control systems to improve vehicle stability have also been studied and published in articles [25], [26], [27], [28]. Some experiments related to the vehicle's rollover stability control have also been conducted in steering and lane-changing conditions. Overall, the results were quite good [29]. In addition, control of the active suspension [30], active steering [31], etc., have brought high efficiency for ensuring the car's stability when moving.

A stabilizer bar also called an anti-roll bar, is another very effective way to prevent a car from rolling [32]. Stabilizer bars are made in many different ways these days. There are usually three main types: the passive (mechanical) stabilizer bar, the active hydraulic stabilizer bar, and the active electronic stabilizer bar. The performance of the passive stabilizer bar is worse than that of the active stabilizer bar. The stabilizer bar can reduce the roll angle when steering and ensure better wheel-to-road interaction [33], [34]. As for the hydraulic stabilizer bars, they are quite complicated and bulky in construction. However, the impact force generated by the hydraulic stabilizer bar is quite large [35]. Therefore, it can ensure stable performance in many situations. The electronic stabilizer bar has a better response rate, but the force generated by the motor is insignificant [36]. According to Gao et al., using a stabilizer bar can affect the stiffness of the suspension, but its use is necessary [37]. In [38], Muniandy et al. introduced using an active stabilizer bar controlled by the PI-PD (Proportional Integral-Proportional Derivative) controller. The parameters of the PI-PD controller are tuned by a simple fuzzy algorithm. According to Tan et al., a robust control algorithm is necessary for hydraulic stabilizer bars used in trucks [39]. The results regarding system stability are evaluated in the frequency domain when comparing AARB (active anti-roll bar) and PARB (passive anti-roll bar) [39]. A control-related experiment for a hydraulic stabilizer bar was performed by Dawei et al. in [35]. According to the results of this experiment, the values associated with rollover oscillations were lower when the active stabilizer bar was used compared to those without the stabilizer bar. The car's oscillating state is constantly changing, so determining the operating conditions for the stabilizer bar is difficult. Therefore, intelligent control algorithms, such as fuzzy algorithms, should replace conventional control algorithms to aid in identifying better-working states. In [40], Nguyen introduced a fuzzy algorithm to control the hydraulic stabilizer bar. This controller is quite simple and has only a single input. Nguyen's study also shows a fuzzy controller with two inputs [41]. Two inputs to this controller include the change in the vehicle body roll angle and the displacement of the unsprung mass. These objects must be handled when the vehicle moves at high speed. In general, these algorithms bring high efficiency to operating the system.

Intending to improve stability and anti-roll when the car is moving at high speed, this article proposes using the active stabilizer bar on both the front and the rear axles of the vehicle. Using a fuzzy controller with one input or two inputs still does not fully satisfy anti-roll conditions. Therefore, the

author recommends using a new controller with three inputs to improve the system's quality. The roll angle, the unsprung mass displacement, and the resistance torque are three inputs to the controller. When the automobile steers, all three parameters change. These values are closely related to the rolling instability of the car. Therefore, it is appropriate to consider these values as input parameters for the controller. These parameters are interdependent in a complex dynamic model. Using a fuzzy algorithm with three inputs to control the active stabilizer bar is unique and novel, considered a new article point. This work uses the numerical simulation method to evaluate the efficiency of the control algorithm. The model of a complex dynamic combined with many other models is also established to describe the car's oscillations when steering. The article's content consists of four main parts: an introduction section, a material section, a results section, and a conclusions section. Specific contents will be presented in the following sections.

II. MATERIAL

A dynamic model needs to be established to simulate car oscillations. Many dynamical models are used for this purpose, such as nonlinear, linear, half models, etc. In this work, the author proposes using a complex model that combines three component models: a spatial oscillation model (Figure 1), a nonlinear motion model (Figure 2), and a nonlinear tire model.

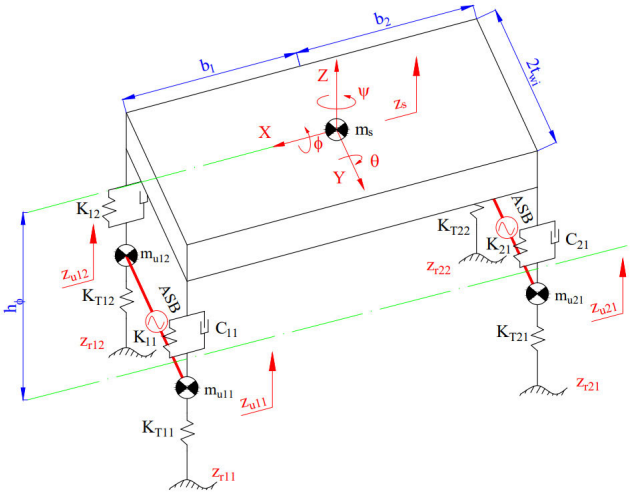

FIGURE 1. A spatial model.

The spatial oscillation model has seven degrees of freedom (Figure 1), corresponding to five masses. The equations describing the oscillation of the car are shown as follows:

$$m_s\ddot{z}_s = \sum_{i,j=1}^{2}\left(F_{Kij} + F_{Cij}\right) \tag{1}$$

$$\left(J_\phi + m_s h_\phi^2\right)\ddot{\phi} = \sum_{i,j=1}^{2}\left((-1)^{j-1}\left(F_{Kij} + F_{Cij}\right)t_{wi}\right) + \left(g sin\phi + a_y cos\phi\right) m_s h_\phi \tag{2}$$

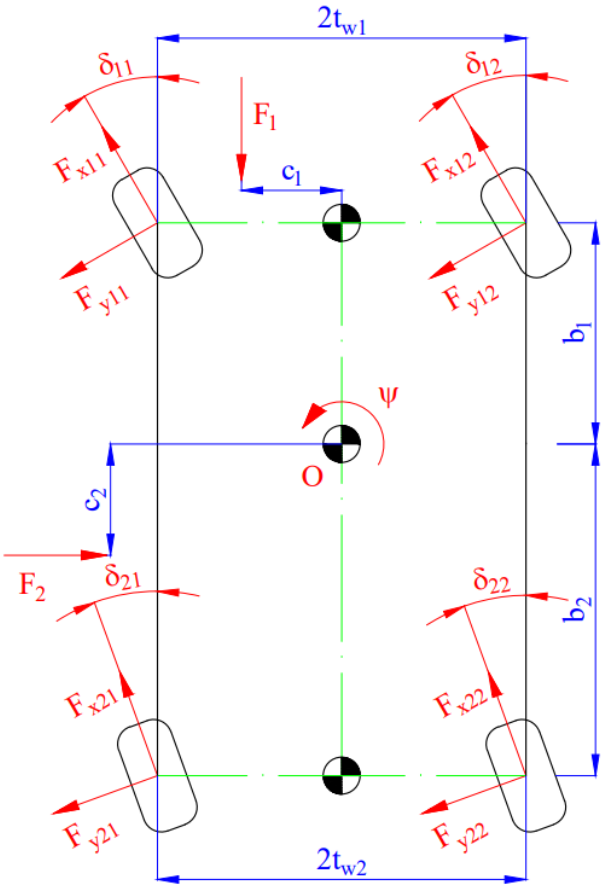

FIGURE 2. A nonlinear model.

$$\left(J_\theta + m_s h_\theta^2\right)\ddot{\theta} = \sum_{i,j=1}^{2}\left((-1)^{i-1}\left(F_{Kij} + F_{Cij}\right)b_i\right) \tag{3}$$

$$m_{uij}\ddot{z}_{uij} = F_{KTij} - F_{Kij} - F_{Cij} + (-1)^j F_{ASBij} \tag{4}$$

The nonlinear motion model has three degrees of freedom (Figure 2), which are used for the three directions of motion. Therefore, it is necessary to establish three differential equations to describe them.

$$\left(m_s + \sum_{i,j=1}^{2} m_{uij}\right)\left(\dot{v}_x - \left(\dot{\alpha} + \dot{\psi}\right)v_y\right) = \sum_{i,j=1}^{2}\left(F_{xij}cos\delta_{ij} - F_{yij}sin\delta_{ij}\right) - F_1 \tag{5}$$

$$\left(m_s + \sum_{i,j=1}^{2} m_{uij}\right)\left(\dot{v}_y + \left(\dot{\alpha} + \dot{\psi}\right)v_x\right) = \sum_{i,j=1}^{2}\left(F_{xij}sin\delta_{ij} + F_{yij}cos\delta_{ij}\right) - F_2 \tag{6}$$

$$J_\psi\ddot{\psi} = \sum_{i,j=1}^{2}\begin{pmatrix}(-1)^j\left(F_{xij}cos\delta_{ij} - F_{yij}sin\delta_{ij}\right)t_{wi} \\ +(-1)^{i+1}\left(F_{xij}sin\delta_{ij} + F_{yij}cos\delta_{ij}\right)b_i \\ +F_i c_i - M_{zij}\end{pmatrix} \tag{7}$$

The wheel forces should be calculated according to the tire model. As for the linear tire models, they are quite simple, and the accuracy is not high. In contrast, nonlinear tire models can provide more accuracy but are quite complex. In this article, a nonlinear tire model called the Pacejka tire model is used. The Pacejka tire model must use many parameters related to the experiment [42]. Wheel forces and moments are complex functions that depend on the slip ratio, the slip angle, the dynamic force, etc. [42].

$$F_x = f\left(F_z, s_x, v\right) \tag{8}$$
$$F_x = f\left(F_z, \alpha, v\right) \tag{9}$$
$$M_z = f\left(F_z, \alpha, v\right) \tag{10}$$

The process of calculating tire forces and moments should be referred to in [43].

A hydraulic actuator is controlled by the controller's voltage signal. The servo valves can move when voltage is supplied to the actuator. Typically, the voltage utilized for the actuator does not exceed 24 volts. The act of opening and closing servo valves will alter the fluid pressure within the hydraulic motor. Consequently, the active stabilizer bar may provide torque to the two arms. The following equations demonstrate its fundamental principle:

$$\dot{X}_{sv}\tau + X_{sv} = K_{sv}u\left(t\right) \tag{11}$$
$$K_{qi}X_{sv} = D_m\dot{\theta}_m + K_{ce}\Delta P + \frac{V_t}{4\beta_e}\Delta\dot{P} \tag{12}$$
$$D_m\Delta P = J_m\ddot{\theta}_m + B_m\dot{\theta}_m + T_r \tag{13}$$

The system diagram is shown in Figure 3. The fuzzy controller has three inputs, including roll angle (the first input), displacement of the unsprung mass (the second input), and resistance torque (the third input). The sensor can obtain the value of the first two inputs directly, while the value of the last input can be calculated indirectly through the vertical force difference at the wheels. The membership function of the fuzzy controller is shown in Figure 4, Figure 5, and Figure 6. These functions are briefly described in the formula (14).

$$\Gamma\left(x, \xi\right) = \begin{cases} 1, & x < \xi_a \\ \dfrac{x-a}{b-a}, & \xi_a \le x \le \xi_b \\ \dfrac{c-x}{c-b}, & \xi_b \le x \le \xi_c \\ 1, & x > \xi_c \end{cases}$$
$$= max\left(min\left(\frac{x-a}{b-a}, \frac{c-x}{c-b}\right), 0\right) \tag{14}$$

The output of membership functions is determined by the following three factors:

+ The system's response time must be quick.

+ As the input values increase, the value of the degree of membership must increase, and vice versa. If the input values are zero, the value of the degree of membership must also be zero.

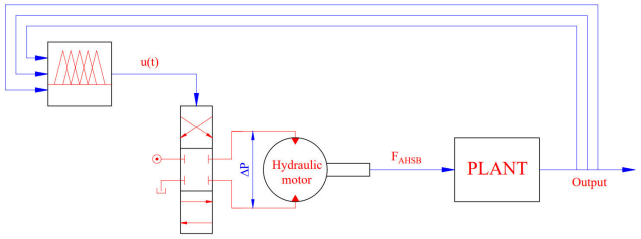

FIGURE 3. The control system diagram.

+ When the input values reach a certain threshold, the degree of membership value should be kept as high as possible.

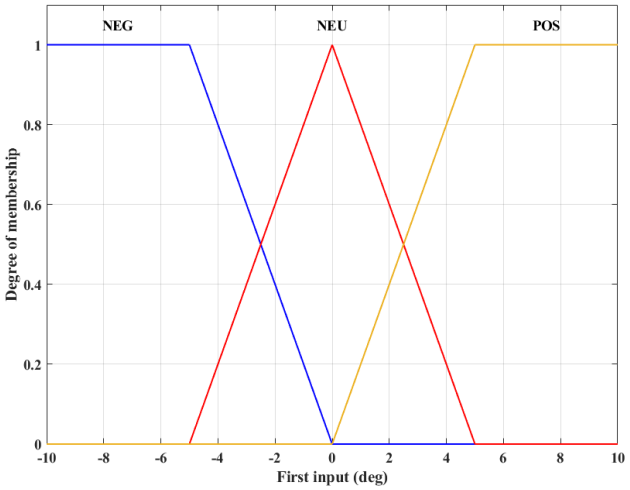

FIGURE 4. Membership function (the first input).

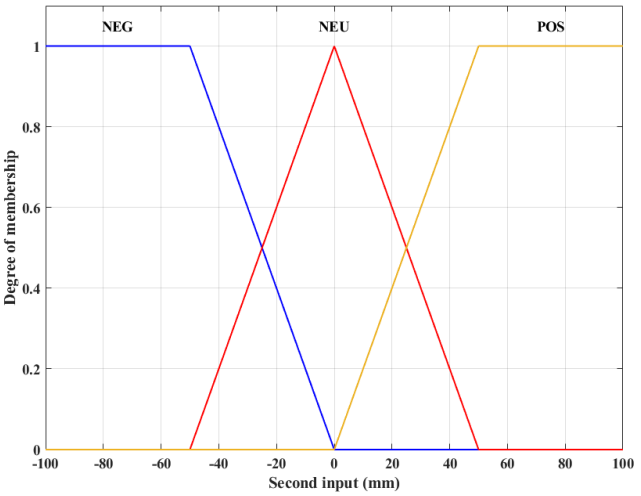

FIGURE 5. Membership function (the second input).

The fuzzy rule is considered the essential element of the defuzzification process. The fuzzy rule, which is shown in Table 1, is designed based on the following points of view:

+ The first point: If the vehicle roll angle is large, the voltage to be generated is large, and vice versa

TABLE 1. Fuzzy rules.

First input	Second input	Third input	Output
NEG	NEG	NEG	VNEG
NEG	NEG	NEU	BNEG
NEG	NEG	POS	SNEG
NEG	NEU	NEG	BNEG
NEG	NEU	NEU	SNEG
NEG	NEU	POS	NEU
NEG	POS	NEG	SNEG
NEG	POS	NEU	NEU
NEG	POS	POS	SPOS
NEU	NEG	NEG	BNEG
NEU	NEG	NEU	SNEG
NEU	NEG	POS	NEU
NEU	NEU	NEG	SNEG
NEU	NEU	NEU	NEU
NEU	NEU	POS	SPOS
NEU	POS	NEG	NEU
NEU	POS	NEU	SPOS
NEU	POS	POS	BPOS
POS	NEG	NEG	SNEG
POS	NEG	NEU	NEU
POS	NEG	POS	SPOS
POS	NEU	NEG	NEU
POS	NEU	NEU	SPOS
POS	NEU	POS	BPOS

TABLE 1. *(Continued.)* **Fuzzy rules.**

POS	POS	NEG	SPOS
POS	POS	NEU	BPOS
POS	POS	POS	VPOS

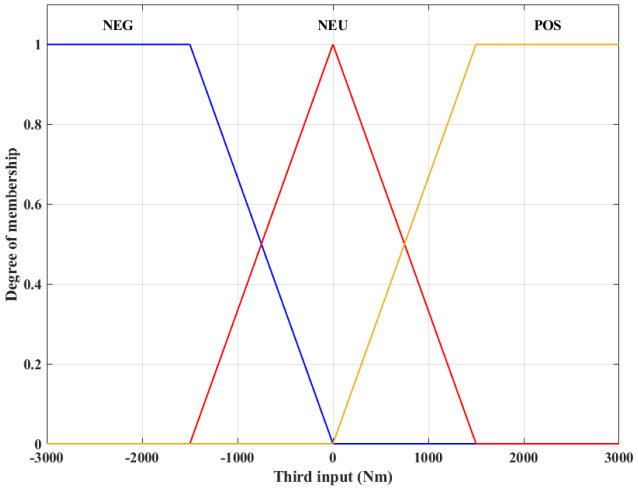

FIGURE 6. Membership function (the third input).

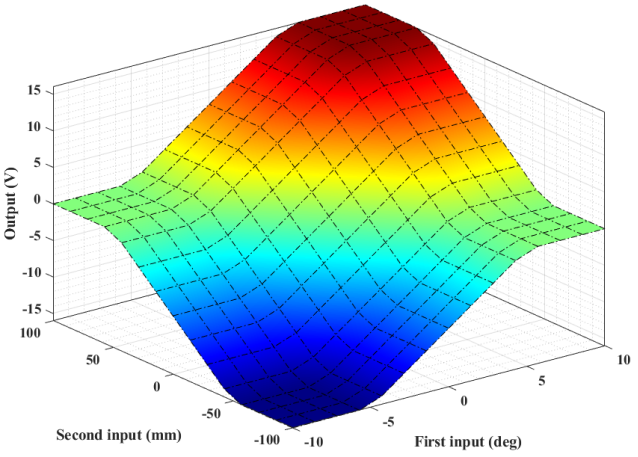

FIGURE 7. The fuzzy surface.

+ The second point: If the unsprung mass displacement is large, the voltage to be generated is large, and vice versa

+ The third point: If the resisting torque is large, the voltage to be generated is large, and vice versa

+ The fourth point: If all inputs are large, the value of the output must also be large, and vice versa

+ The fifth point of view: If the level of input values is different, the output value must be selected appropriately to ensure the stability of the car.

Based on three input levels, a result combination of 27 output cases is given in Table 1. These rules are more intuitively described by a fuzzy surface in the Figure 7.

The abbreviations listed in Table 1 include:

BNEG: big negative
BPOS: big positive
NEG: negative
NEU: neutral
POS: positive
SNEG: small negative
SPOS: small positive
VNEG: very big negative
VPOS: very big positive

III. RESULTS

A. CONDITIONS

The simulation is performed by MATLAB application under specific conditions. The technical parameters of the reference vehicle are shown in Table 2.

TABLE 2. The technical parameters.

Description	Symbol	Unit	Value
Vehicle sprung mass	m_u	kg	1810
Vehicle unsprung mass	m_s	kg	50
Distance from the CG to the RA	h_θ	mm	560
Distance from the CG to the PA	h_φ	mm	540
Distance from CG to the axle	b	mm	725/720
Half of the track width	t_w	mm	730/725
Inertia moment (longitudinal)	J_x	kgm^2	690
Inertia moment (lateral)	J_y	kgm^2	2810
Inertia moment (vertical)	J_z	kgm^2	2780
Pressure coefficient	K_{ce}	$m^5N^{-1}s^{-1}$	4×10^{-11}
Gain coefficient	K_{qi}	m^2s^{-1}	2×10^{-2}
Valve coefficient	K_v	mA^{-1}	3×10^{-2}
Effective bulk modulus	β_e	Nm^{-2}	6×10^{6}
Inertia moment (motor)	J_m	kgm^2	35×10^{-1}
Friction coefficient	B_m	$Nmsrad^{-1}$	10
Flow per revolution	D_m	$lrad^{-1}$	1.5×10^{-2}
Total volume of trapped oil	V_t	l	1
Time constant	τ	ms	5

This work uses a J-turn steering angle to simulate car oscillation. The change of steering angle with time is shown in Figure 8.

In each case, the results corresponding to the situations should be compared. There are four situations to consider when comparing results, including:

+ Active with Fuzzy: the car uses active stabilizer bars controlled by a new fuzzy algorithm designed in this article.

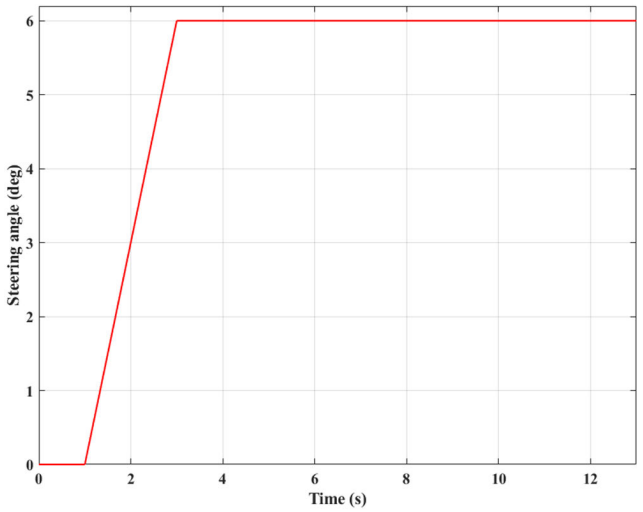

FIGURE 8. Steering angle.

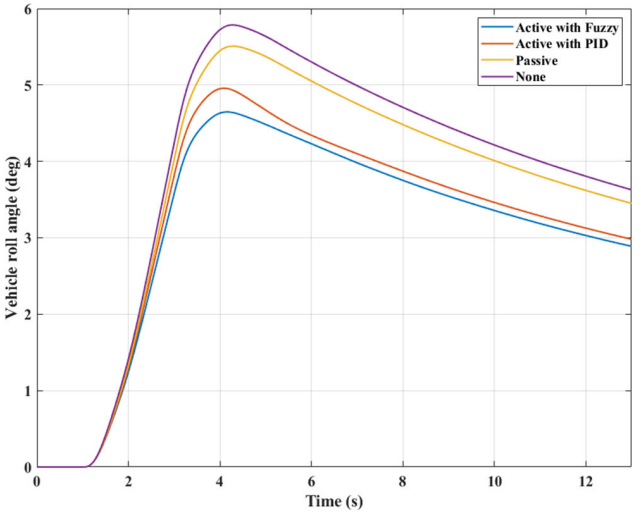

FIGURE 9. Vehicle roll angle (1st case).

+ Active with PID: the car uses active stabilizer bars controlled by a traditional PID algorithm. The parameters of the PID controller are determined by the Ziegler-Nichols method.

+ Passive: the car uses passive stabilizer bars (also known as mechanical stabilizer bars).

+ None: the car does not have any stabilizer bars.

B. RESULT AND DISCUSSION

The results obtained from the simulation are divided into three cases, corresponding to three different speed values: $v_1 = 65$ (km/h); $v_2 = 75$ (km/h); $v_3 = 85$ (km/h).

1) 1st CASE

In the first case, the speed that is used for simulation is not high, $v_1 = 65$ (km/h). The change in the roll angle in the time domain is depicted in Figure 9. According to this result, the roll angle of the car body increases from zero up to its maximum value, reaching 5.79°, 5.51°, 4.96°, and 4.64° (in order: None, Passive, Active with PID, and Active with Fuzzy, respectively). The value of the roll angle peaks shortly after the steering angle has reached its maximum. The reason for this is because of the vehicle's inertia when moving. These values peak at different times with a relatively small-time difference. The vehicle's roll angle will peak first when using the active stabilizer bar controlled by the fuzzy algorithm. In contrast, the value of the vehicle situation without the stabilizer bar will peak last. After the vehicle body roll angles have reached their maximum values, they will gradually decrease over time, although the steering angle remains stable. This is caused by the nonlinear tire model used in this work. Compared with the conventional linear tire model, the nonlinear tire model more fully describes the characteristics of elastic tire deformation. According to this result, the value of the lateral force will decrease when the steering angle is maintained, reducing the roll angle's value.

Changing the roll angle will also cause the vertical force at the wheels to change. If these values are further reduced, the interaction between the wheels and the road surface will also be negatively affected. Once they approach zero, the rollover phenomenon can occur quickly. The change in the dynamic force in the vehicle's situation using the active stabilizer bar with the fuzzy algorithm is clearly shown in Figure 10. Because the body is tilted outward when steering, the vertical force of the outer wheel will increase (F_{z12} and F_{z22}), while the vertical force of the inner wheel will decrease (F_{z11} and F_{z21}). According to this finding, the minimum value of the dynamic force at the inner wheel at the rear axle is only $F_{z21} = 3628.6$ (N), which has decreased by 649.5 (N) compared to the initial state. When the steering angle is maintained, the roll angle will decrease gradually (this was explained above), so the difference in the vertical force between the two wheels will also decrease gradually.

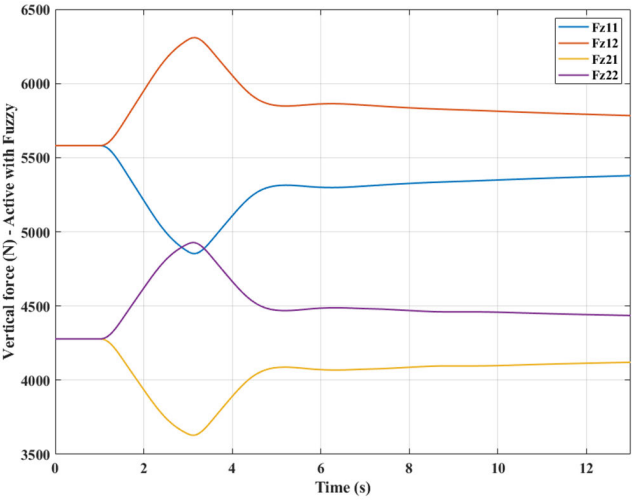

FIGURE 10. Vertical force - active with fuzzy (1st case).

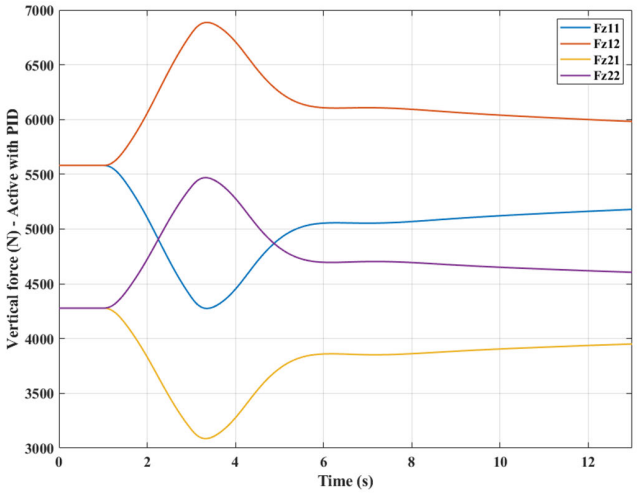

FIGURE 11. Vertical force - active with PID (1st case).

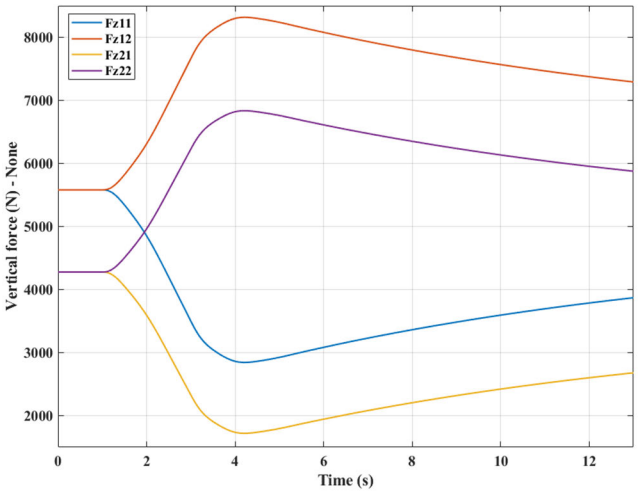

FIGURE 13. Vertical force - none (1st case).

The system's performance will be worse if only the PID algorithm is used to control the active stabilizer bar instead of the fuzzy algorithm with three inputs. Looking at Figure 11, one can see that the change in dynamic force at the wheels is more significant. The attenuation of these values can be up to 1305.7 (N) for the front wheels and 1191.0 (N) for the rear wheels. The minimum value of the wheel's vertical force in position (21) will be lower than the above situation, only 3087.1 (N). However, this reduction is insignificant, and the car can still operate normally.

Figure 12 shows that when a car only has a passive stabilizer bar, the dynamic forces on the wheels are reduced even more than in two situations above. The vertical force of the rear wheel is reduced sharply to only 2271.2 (N), while the front wheel is declined to 3416.7 (N). The difference in the dynamic values of the wheels when steering compared to the equilibrium state is also more considerable, reaching 2164.5 (N) and 2006.9 (N), respectively, for the front and the rear wheels.

For the last situation, if the car does not have a stabilizer bar, the attenuation of wheel dynamics will be most significant during steering (Figure 13). The value of F_{z21} suddenly dropped sharply to only 1720.5 (N), decreasing by 2557.6 (N) compared to the initial state before steering. This increases the risk of unstable situations, such as a rollover.

Once the roll angle increases, so do the vehicle's rollover index. This indicator is determined by the difference in the vertical forces of the wheels. Based on the results shown in Figure 14, the maximum roll index of the car belongs to the situation where the vehicle does not have a stabilizer bar, RI = 0.60. These values decrease in order from Passive (RI = 0.47), Active with PID (RI = 0.28), and Active with Fuzzy (RI = 0.15). These results show the vehicle can operate safely at $v_1 = 65$ (km/h). As a result, increasing the speed to investigate the car's stability when steering is necessary. This process will continue to be performed in the second case.

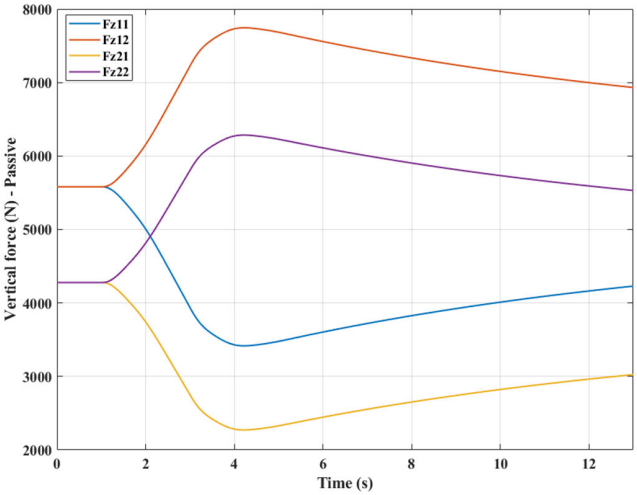

FIGURE 12. Vertical force - Passive (1st case).

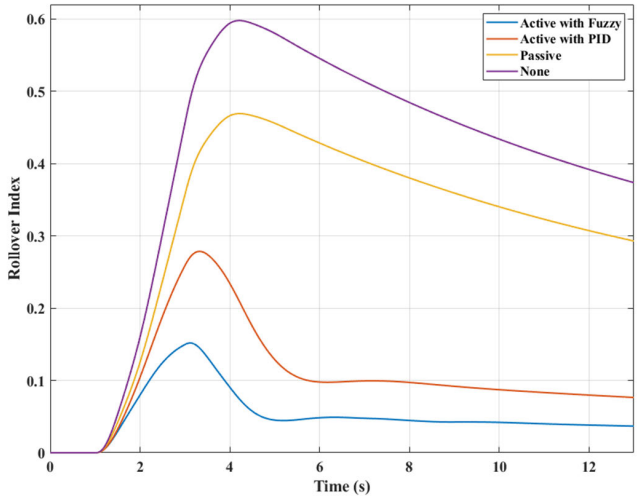

FIGURE 14. Rollover index (1st case).

TABLE 3. Simulation results (1st case).

	Maximum roll angle (°)	Maximum rollover index	Minimum vertical force (N)	Maximum difference of dynamic force (N) front – rear
Active with Fuzzy	4.64	0.15	3628.6	727.8 – 649.5
Active with PID	4.96	0.28	3087.1	1305.7 – 1191.0
Passive	5.51	0.47	2271.2	2164.5 – 2006.9
None	5.79	0.60	1720.5	2734.9 – 2557.6

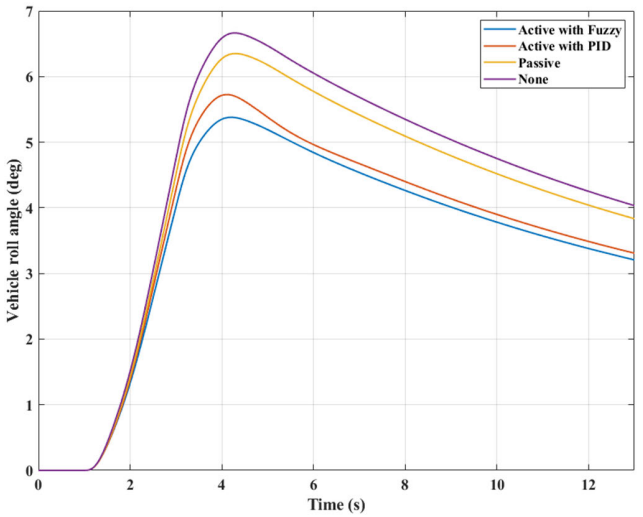

FIGURE 15. Vehicle roll angle (2nd case).

The simulation results of the first case are summarized in Table 3.

2) 2nd CASE

In the second case, the car's speed increases to $v_2 = 75$ (km/h). This is a rather significant value, so the car's instability when steering is greater than in the first case. Similar to the first case, the outputs of the simulation problem still include the change of the roll angle, the change of dynamic force, and rollover index.

Figure 15 depicts the car's roll angle changing during the simulation. The trend of these values is similar to the first case. The only difference is that the magnitude of the values has increased more. The peak values of the roll angles obtained are 6.66°, 6.35°, 5.72°, and 5.38°, respectively, corresponding to four situations. Compared to the case above, these values have increased by more than 15%. Because the roll angle of the car body has increased more sharply, the difference in vertical forces at the wheels will also change more. This is demonstrated by Figure 16, Figure 17, Figure 18, and Figure 19.

According to the results from Figure 16, the vertical force of the wheel (21) has been reduced to 3532.2 (N). This result

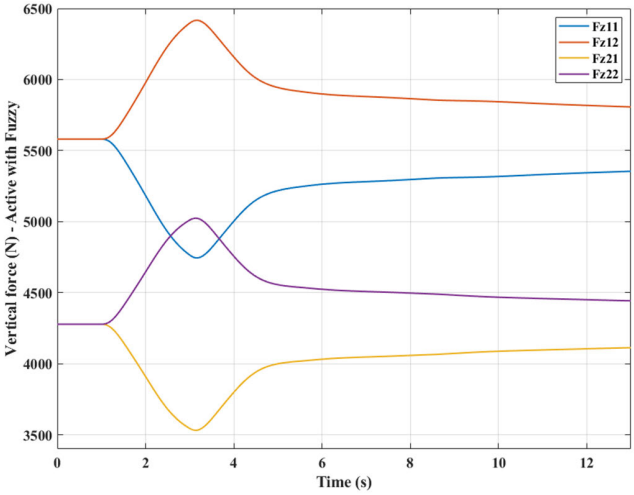

FIGURE 16. Vertical force - active with fuzzy (2nd case).

is achieved when the vehicle uses the active stabilizer bar with the fuzzy algorithm. So, this change is relatively small. The difference in dynamic force can be increased even more if the PID algorithm is used to control the hydraulic stabilizer bar instead of the intelligent algorithm, which can be clearly observed in Figure 17. According to the findings, the values of the vertical forces of the front and rear wheels are reduced by 1495.5 (N) and 1364.2 (N), respectively. This declines the dynamic force of the wheel (21) to 2913.9 (N). This decrease is more significant than the situation mentioned above.

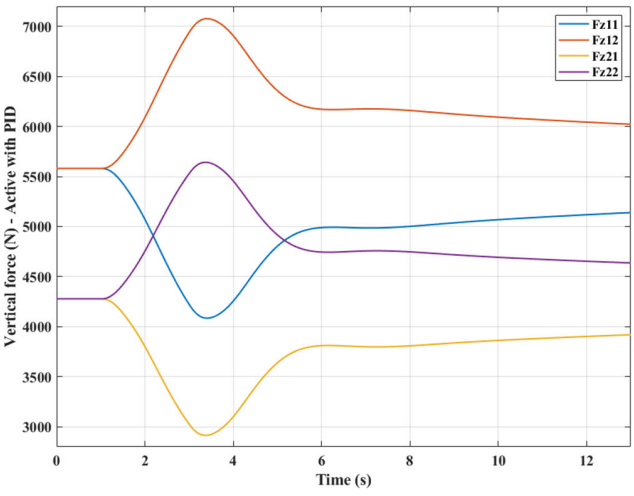

FIGURE 17. Vertical force - active with PID (2nd case).

A substantial reduction in the dynamic force of the wheels is shown in Figure 18. This is due to the fact that cars only have passive stabilizer bars and not active stabilizer bars. The minimum value of the dynamic force has suddenly decreased to no more than 1964.4 (N), only 55.61% of that of a car using hydraulic stabilizer bars controlled by an intelligent algorithm with three inputs. In this situation, the change in dynamic force is also more considerable, reaching 2495.0 (N)

and 2313.7 (N), which correspond to the front and rear axles of the vehicle, respectively. Finally, a more drastic change in the dynamic force occurs when the car does not have the stabilizer bar (this is demonstrated in Figure 19). The vertical force of the rear wheel has been reduced from 4278.1 (N) to 1332.1 (N), a loss of 68.86% from the initial steady state. There is a greater risk of car roll instability with this attenuation. If the vehicle's speed keeps increasing, the wheel's vertical force can decrease even more.

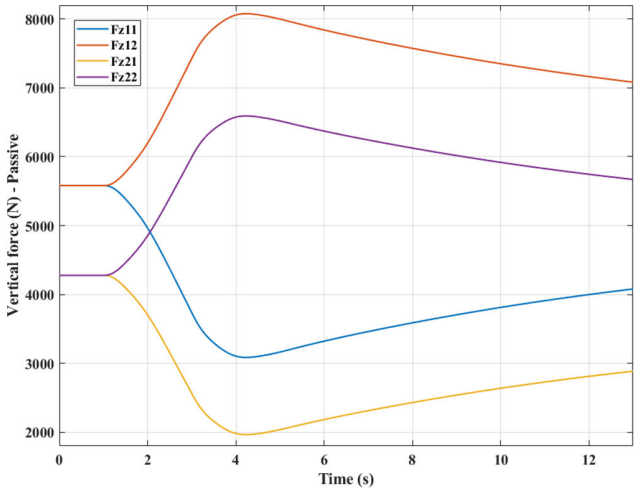

FIGURE 18. Vertical force - passive (2nd case).

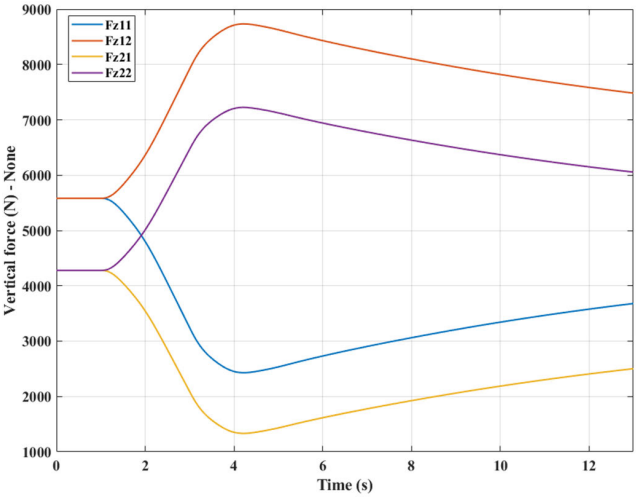

FIGURE 19. Vertical force - none (2nd case).

In the second case, the change in the rollover index over time is more significant than in the first case (Figure 20). The risk of a rollover can be as high as 69% if the vehicle is not equipped with the stabilizer bar. This risk drops to 54% once mechanical stabilizer bars are used on the vehicle's front and rear axles. If cars use hydraulic stabilizer bars controlled by automatic controllers, the risk of rolling over can be drastically reduced to only 17% (Active with Fuzzy) and 32% (Active with PID).

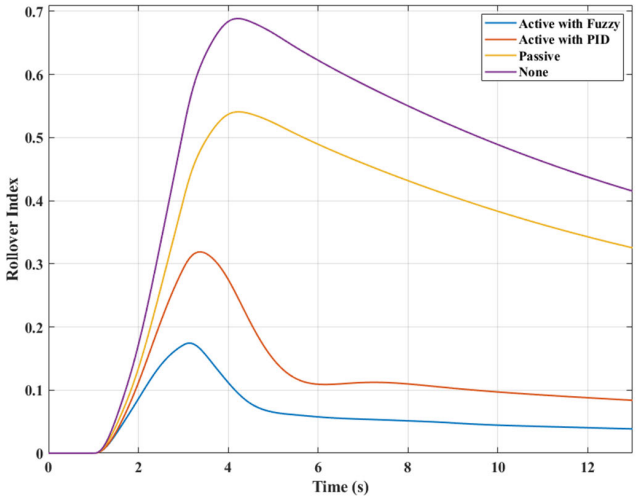

FIGURE 20. Rollover index (2nd case).

These simulation results are presented in full in Table 4.

TABLE 4. Simulation results (2nd case).

	Maximum roll angle (°)	Maximum rollover index	Minimum vertical force (N)	Maximum difference of dynamic force (N) front – rear
Active with Fuzzy	5.38	0.17	3532.2	835.9 – 745.9
Active with PID	5.72	0.32	2913.9	1495.9 – 1364.2
Passive	6.35	0.54	1964.4	2495.0 – 2313.7
None	6.66	0.69	1332.1	3151.9 – 2946.0

3) 3rd CASE

In the last case, the car's speed increases to a very high level, $v_3 = 85$ (km/h). The parameters' variation, shown above, will be more significant.

According to simulation results, the vehicle's roll angle peaked at 7.44°, 7.10°, 6.42°, and 6.07°, corresponding to four situations: None, Passive, Active with PID, and Active with Fuzzy (Figure 21). These values have increased by about 30% compared to the first case. In general, the roll angle of the car body is quite significant if the vehicle does not have stabilizer bars. The difference between the first situation (None) and the last situation (Active with Fuzzy) can be up to 1.37°, accounting for 22.57% of the difference compared to the last situation.

The fuzzy algorithm with three inputs improves the system's performance. This is demonstrated by the change in wheel dynamic force in Figure 22 and Figure 23. It can be seen clearly that the change in dynamic force is smaller if the fuzzy algorithm is used instead of the PID algorithm. The attenuation of the dynamic force at the wheel is also more

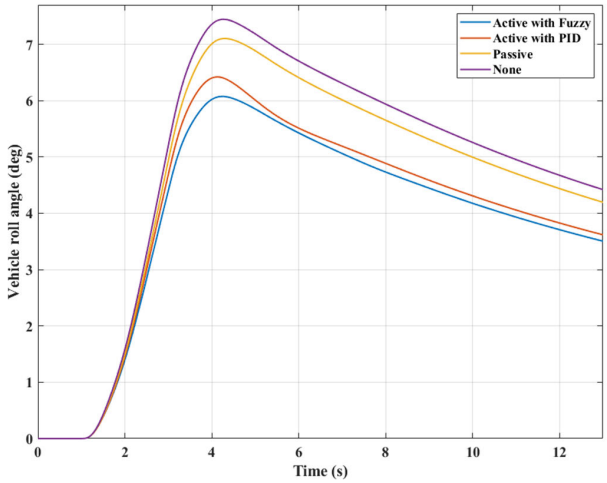

FIGURE 21. Vehicle roll angle (3rd case).

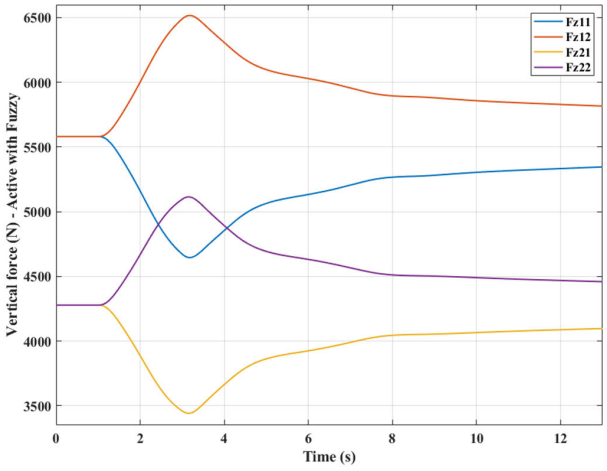

FIGURE 22. Vertical force - active with fuzzy (3rd case).

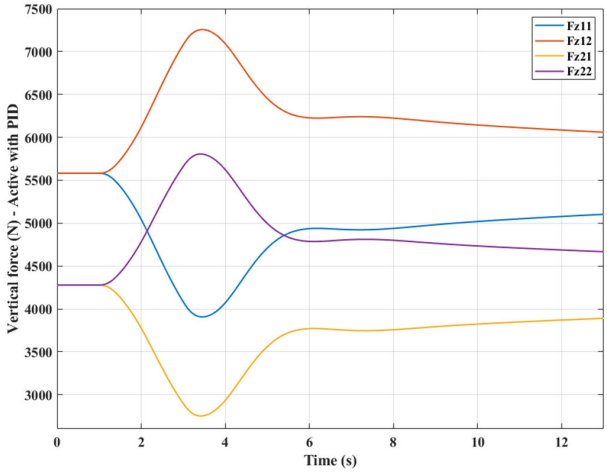

FIGURE 23. Vertical force - active with PID (3rd case).

negligible, reaching only 3441.9 (N) for the case using the fuzzy algorithm and 2751.4 (N) for the remaining situation. Besides, the convergence of these values when using the fuzzy algorithm is better than that of PID.

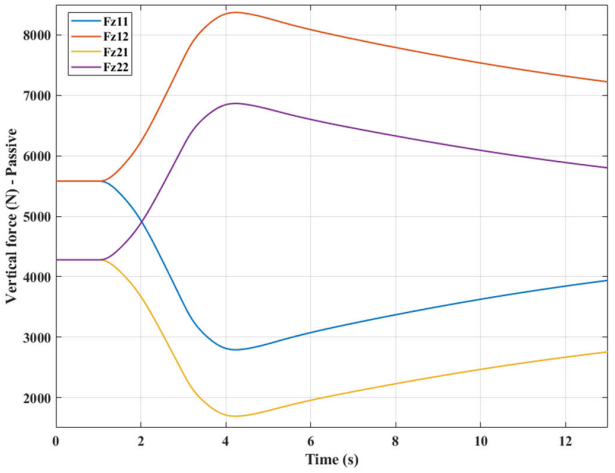

FIGURE 24. Vertical force - passive (3rd case).

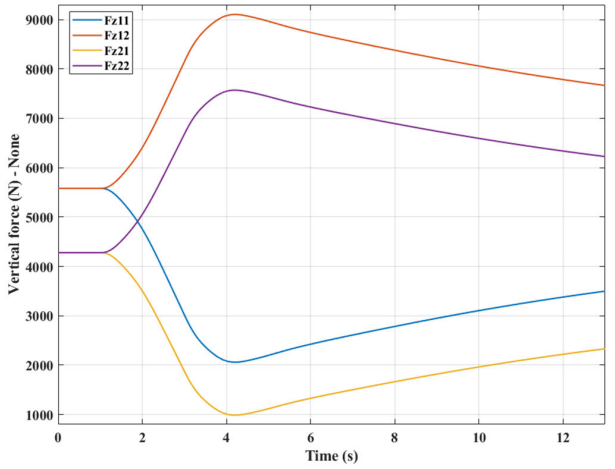

FIGURE 25. Vertical force - none (3rd case).

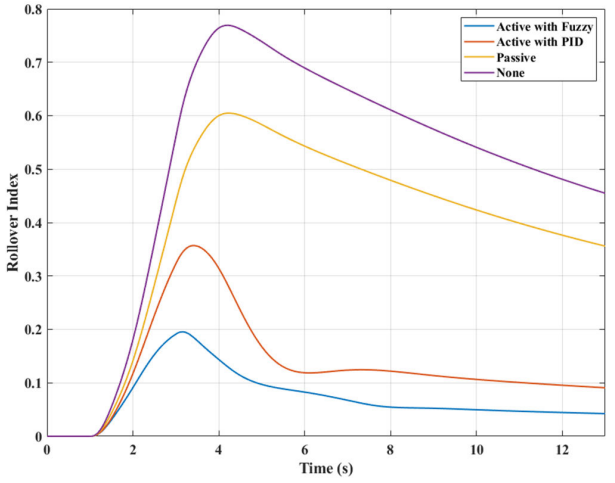

FIGURE 26. Rollover Index - None (3rd case).

In a situation where the vehicle uses only mechanical stabilizer bars (Figure 24) or no stabilizer bars (Figure 25), the dynamic force of the wheels will be reduced

more strongly. The minimum value they achieve is only about 1690.8 (N) and 988.0 (N). These relatively low numbers show that the car might not be stable if the speed or the steering angle keeps going up.

The car's rollover index also increased with the drastic reduction of the wheels' dynamic force (Figure 26). The peak value of the rollover index is up to 0.77 when the vehicle is not using any stabilizer bars. Meanwhile, this value decreases by 0.60 if the mechanical stabilizer bar is used. This value can be reduced even more to 0.36 and 0.19 once active stabilizer bars are fitted at the front and rear axles of the car. Obviously, the risk of rolling over is four times higher if the vehicle does not use the stabilizer bar (compared to using the stabilizer bar with the fuzzy algorithm).

Table 5 summarizes the main results of the simulation of the last case.

TABLE 5. Simulation results (3rd case).

	Maximum roll angle (°)	Maximum rollover index	Minimum vertical force (N)	Maximum difference of dynamic force (N) front – rear
Active with Fuzzy	6.07	0.19	3441.9	935.5 – 836.2
Active with PID	6.42	0.36	2751.4	1674.4 – 1526.7
Passive	7.10	0.60	1690.8	2790.4 – 2587.3
None	7.44	0.77	988.0	3520.7 – 3290.1

IV. CONCLUSION

Under the influence of centrifugal force, the vehicle body may be tilted when steering. The roll angle of the car body causes the difference in the dynamic forces on the wheels. If this change is too significant, the risk of a rollover will also increase. In this research, the solution of using the active stabilizer bar is proposed to reduce the rollover angle and rollover index of the car when steering. A complex dynamic model has been designed to simulate car oscillations. In addition, a fuzzy algorithm with three inputs has also been established to control the operation of the active stabilizer bar.

The simulation is performed by MATLAB® software in the time domain. Three cases are to be made, corresponding to three specific velocity values. In each case, four scenarios are considered. According to research, using the active stabilizer bar under the control of a fuzzy algorithm with three inputs can significantly reduce the car's roll angle. Besides, the attenuation of wheel dynamics is also less in this situation. This leads to a reduction in the rollover index of the car when steering, i.e., limiting the phenomenon of rolling over. As the vehicle's speed increases, these values increase accordingly. Under the operation of a fuzzy algorithm with three inputs, the performance of the hydraulic stabilizer bar is always guaranteed to be the best.

This work has only involved calculations and simulations, so some practical factors have not been fully considered. In the future, some experiments can be carried out to comprehensively evaluate the control system's quality for the stabilizer bar. Also, the fuzzy algorithm with three inputs should be combined with other intelligent control algorithms to improve system performance.

REFERENCES

[1] D. N. Nguyen, M. P. Le, T. A. Nguyen, T. B. Hoang, T. T. H. Tran, and N. D. Dang, "Enhancing the stability and safety of vehicle when steering by using the active stabilizer bar," *Math. Problems Eng.*, vol. 2022, pp. 1–10, Jun. 2022, doi: 10.1155/2022/5617167.

[2] Z. Zakaria, M. S. O. Baslasl, A. Samsuri, I. Ismail, A. Supee, and N. B. Haladin, "Rollover phenomenon in liquefied natural gas storage tank," *J. Failure Anal. Prevention*, vol. 19, no. 5, pp. 1439–1447, Oct. 2019, doi: 10.1007/s11668-019-00739-2.

[3] G. Azimi, A. Rahimi, H. Asgari, and X. Jin, "Severity analysis for large truck rollover crashes using a random parameter ordered logit model," *Accident Anal. Prevention*, vol. 135, Feb. 2020, Art. no. 105355, doi: 10.1016/j.aap.2019.105355.

[4] S. Liu, W. D. Fan, and Y. Li, "Injury severity analysis of rollover crashes for passenger cars and light trucks considering temporal stability: A random parameters logit approach with heterogeneity in mean and variance," *J. Saf. Res.*, vol. 78, pp. 276–291, Sep. 2021, doi: 10.1016/j.jsr.2021.06.013.

[5] A. Brandt, B. Jacobson, and S. Sebben, "High speed driving stability of road vehicles under crosswinds: An aerodynamic and vehicle dynamic parametric sensitivity analysis," *Vehicle Syst. Dyn.*, vol. 60, no. 7, pp. 2334–2357, Jul. 2022, doi: 10.1080/00423114.2021.1903516.

[6] X. Zhang, Y. Yan, K. Guo, Y. Yang, and G. He, "Vehicle roll centre estimation with transient dynamics via roll rate," *Vehicle Syst. Dyn.*, vol. 60, no. 2, pp. 699–717, Feb. 2022, doi: 10.1080/00423114.2020.1838565.

[7] L. Tian, Y. Li, J. Li, and W. Lv, "A simulation based large bus side slip and rollover threshold study in slope-curve section under adverse weathers," *PLoS ONE*, vol. 16, no. 8, Aug. 2021, Art. no. e0256354, doi: 10.1371/journal.pone.0256354.

[8] N. Ikhsan, A. Saifizul, and R. Ramli, "The effect of vehicle and road conditions on rollover of commercial heavy vehicles during cornering: A simulation approach," *Sustainability*, vol. 13, no. 11, p. 6337, 2021, doi: 10.3390/su13116337.

[9] Y. Yin, H. Wen, L. Sun, and W. Hou, "The influence of road geometry on vehicle rollover and skidding," *Int. J. Environ. Res. Public Health*, vol. 17, no. 5, p. 1648, Mar. 2020, doi: 10.3390/ijerph17051648.

[10] T. A. Nguyen, "Control the hydraulic stabilizer bar to improve the stability of the vehicle when steering," *Math. Model. Eng. Problems*, vol. 8, no. 2, pp. 199–206, Apr. 2021, doi: 10.18280/mmep.080205.

[11] T. A. Nguyen, "Determination of the rollover limitation of a vehicle when moving by 4-dimensional plots," *Adv. Syst. Sci. Appl.*, vol. 22, no. 3, pp. 96–105, 2022, doi: 10.25728/assa.2022.22.3.1258.

[12] D. N. Nguyen, T. A. Nguyen, T. B. Hoang, and N. D. Dang, "Establishing the method to predict the limited roll angle of the vehicle based on the basic dimensions," *Math. Model. Eng. Problems*, vol. 8, no. 5, pp. 775–779, Oct. 2021, doi: 10.18280/mmep.080513.

[13] S. Blume, P. M. Sieberg, N. Maas, and D. Schramm, "Neural roll angle estimation in a model predictive control system," in *Proc. IEEE Intell. Transp. Syst. Conf. (ITSC)*, Oct. 2019, pp. 1625–1630, doi: 10.1109/ITSC.2019.8917106.

[14] A. Tota, L. Dimauro, F. Velardocchia, G. Paciullo, and M. Velardocchia, "An intelligent predictive algorithm for the anti-rollover prevention of heavy vehicles for off-road applications," *Machines*, vol. 10, no. 10, p. 835, Sep. 2022, doi: 10.3390/machines10100835.

[15] M. J. L. Boada, B. L. Boada, and H. Zhang, "Event-triggering H_∞-based observer combined with NN for simultaneous estimation of vehicle sideslip and roll angles with network-induced delays," *Nonlinear Dyn.*, vol. 103, pp. 2733–2752, Feb. 2021, doi: 10.1007/s11071-021-06269-7.

[16] Y. Sellami, H. Imine, A. Boubezoul, and J.-C. Cadiou, "Rollover risk prediction of heavy vehicles by reliability index and empirical modelling," *Vehicle Syst. Dyn.*, vol. 56, no. 3, pp. 385–405, Mar. 2018, doi: 10.1080/00423114.2017.1381980.

[17] S. Tian, L. Wei, C. Schwarz, W. Zhou, Y. Jiao, and Y. Chen, "An earlier predictive rollover index designed for bus rollover detection and prevention," *J. Adv. Transp.*, vol. 2018, pp. 1–10, Nov. 2018, doi: 10.1155/2018/2713868.

[18] M. Ataei, A. Khajepour, and S. Jeon, "Model predictive rollover prevention for steer-by-wire vehicles with a new rollover index," *Int. J. Control*, vol. 93, no. 1, pp. 140–155, Jan. 2020, doi: 10.1080/00207179.2018.1535198.

[19] W. Zhao, L. Ji, and C. Wang, "H_∞ control of integrated rollover prevention system based on improved lateral load transfer rate," *Trans. Inst. Meas. Control*, vol. 41, no. 3, pp. 859–874, Feb. 2019, doi: 10.1177/0142331218773527.

[20] D. Shin, S. Woo, and M. Park, "Rollover index for rollover mitigation function of intelligent commercial vehicle's electronic stability control," *Electronics*, vol. 10, no. 21, p. 2605, Oct. 2021, doi: 10.3390/electronics10212605.

[21] C. Wang, Z. Wang, L. Zhang, D. Cao, and D. G. Dorrell, "A vehicle rollover evaluation system based on enabling state and parameter estimation," *IEEE Trans. Ind. Informat.*, vol. 17, no. 6, pp. 4003–4013, Jun. 2021, doi: 10.1109/TII.2020.3012003.

[22] W. Sun, X. Wang, and C. Zhang, "A model-free control strategy for vehicle lateral stability with adaptive dynamic programming," *IEEE Trans. Ind. Electron.*, vol. 67, no. 12, pp. 10693–10701, Dec. 2020, doi: 10.1109/TIE.2019.2958308.

[23] Z. Jin, J. Li, H. Wang, J. Li, and C. Huang, "Rollover prevention and motion planning for an intelligent heavy truck," *Chin. J. Mech. Eng.*, vol. 34, no. 1, Dec. 2021, doi: 10.1186/s10033-021-00605-z.

[24] M. Dong, Y. Fan, D. Yu, and Q. Wang, "Research on electric vehicle rollover prevention system based on motor speed control," *World Electr. Vehicle J.*, vol. 12, no. 4, p. 195, Oct. 2021, doi: 10.3390/wevj12040195.

[25] S. Rahimi and M. Naraghi, "Design of an integrated control system to enhance vehicle roll and lateral dynamics," *Trans. Inst. Meas. Control*, vol. 40, no. 5, pp. 1435–1446, Mar. 2018, doi: 10.1177/0142331216685389.

[26] F. Lin, S. Wang, Y. Zhao, and Y. Cai, "Research on autonomous vehicle path tracking control considering roll stability," *Proc. Inst. Mech. Eng., D, J. Automobile Eng.*, vol. 235, no. 1, pp. 199–210, 2021, doi: 10.1177/0954407020942006.

[27] S. Yim, "Active roll stabilization with disturbance feedforward control," *IEEE Access*, vol. 9, pp. 19788–19799, 2021, doi: 10.1109/ACCESS.2021.3054837.

[28] Z. Wang, Y. Qin, C. Hu, M. Dong, and F. Li, "Fuzzy observer-based prescribed performance control of vehicle roll behavior via controllable damper," *IEEE Access*, vol. 7, pp. 19471–19487, 2019, doi: 10.1109/ACCESS.2019.2896588.

[29] M. Jalali, E. Hashemi, A. Khajepour, S.-K. Chen, and B. Litkouhi, "Model predictive control of vehicle roll-over with experimental verification," *Control Eng. Pract.*, vol. 77, pp. 95–108, Aug. 2018, doi: 10.1016/j.conengprac.2018.04.008.

[30] D. N. Nguyen and T. A. Nguyen, "A novel hybrid control algorithm sliding mode-PID for the active suspension system with state multivariable," *Complexity*, vol. 2022, pp. 1–14, Jun. 2022, doi: 10.1155/2022/9527384.

[31] X. Ma, P. K. Wong, J. Zhao, and Z. Xie, "Cornering stability control for vehicles with active front steering system using T-S fuzzy based sliding mode control strategy," *Mech. Syst. Signal Process.*, vol. 125, pp. 347–364, Jun. 2019, doi: 10.1016/j.ymssp.2018.05.059.

[32] D. N. Nguyen, N. D. Dang, T. T. H. Tran, T. B. Hoang, and T. A. Nguyen, "Effect of the passive stabilizer bar on the vehicle's stability," *Model. Simul. Eng.*, vol. 2022, pp. 1–8, May 2022, doi: 10.1155/2022/5523012.

[33] H.-G. Park, K.-H. Jeong, M.-K. Park, S.-H. Lee, and K.-K. Ahn, "Electro hydrostatic actuator system based on active stabilizer system for vehicular suspension systems," *Int. J. Precis. Eng. Manuf.*, vol. 19, no. 7, pp. 993–1001, Jul. 2018, doi: 10.1007/s12541-018-0117-9.

[34] H.-Y. Hwang, T.-S. Lan, and J.-S. Chen, "Developing a strategy to improve handling behaviors of a medium-size electric bus using active anti-roll bar," *Symmetry*, vol. 12, no. 8, p. 1334, Aug. 2020, doi: 10.3390/sym12081334.

[35] P. Dawei, K. Zhenxing, W. Xianhui, W. Hongliang, and C. Shan, "Design and experimental validation of control algorithm for vehicle hydraulic active stabilizer bar system," *Proc. Inst. Mech. Eng., D, J. Automobile Eng.*, vol. 233, no. 5, pp. 1280–1295, Apr. 2019, doi: 10.1177/0954407018770539.

[36] Y. Zhang, L. Wang, and R. Xia, "Sliding mode control of electrical active roll stabilizer using switched reluctance motor," SAE Tech. Paper 2018-01-0832, 2018, doi: 10.4271/2018-01-0832.

[37] J. Gao, F. Wu, and Z. Li, "Study on the effect of stiffness matching of anti-roll bar in front and rear of vehicle on the handling stability," *Int. J. Automot. Technol.*, vol. 22, no. 1, pp. 185–199, Feb. 2021, doi: 10.1007/s12239-021-0019-1.

[38] V. Muniandy, P. M. Samin, and H. Jamaluddin, "Application of a self-tuning fuzzy PI–PD controller in an active anti-roll bar system for a passenger car," *Vehicle Syst. Dyn.*, vol. 53, no. 11, pp. 1641–1666, Nov. 2015, doi: 10.1080/00423114.2015.1073336.

[39] V. V. Tan, O. Sename, and P. Gáspár, "Improving roll stability of tractor semi-trailer vehicles by using H_∞ active anti-roll bar control system," *Proc. Inst. Mech. Eng., D, J. Automobile Eng.*, vol. 235, no. 14, pp. 3509–3520, Dec. 2021, doi: 10.1177/09544070211013949.

[40] T. A. Nguyen, "Improving the stability of the passenger vehicle by using an active stabilizer bar controlled by the fuzzy method," *Complexity*, vol. 2021, pp. 1–20, Dec. 2021, doi: 10.1155/2021/6569298.

[41] T. A. Nguyen, "Preventing the rollover phenomenon of the vehicle by using the hydraulic stabilizer bar controlled by a two-input fuzzy controller," *IEEE Access*, vol. 9, pp. 129168–129177, 2021, doi: 10.1109/ACCESS.2021.3114023.

[42] H. B. Pacejka, *Tire and Vehicle Dynamics*, 3rd ed. Oxford, U.K.: Butterworth-Heinemann, 2012, doi: 10.1016/C2010-0-68548-8.

[43] D. N. Nguyen and T. A. Nguyen, "Investigate the relationship between the vehicle roll angle and other factors when steering," *Model. Simul. Eng.*, vol. 2023, pp. 1–15, Jan. 2023, doi: 10.1155/2023/6069078.